

# PROCEEDINGS OF SPIE

[SPIDigitalLibrary.org/conference-proceedings-of-spie](https://SPIDigitalLibrary.org/conference-proceedings-of-spie)

## III-V/silicon photonic integrated circuits for spectroscopic sensing in the 2 $\mu$ m wavelength range

Ruijun Wang, Muhammad Muneeb, Anton Vasiliev, Aditya Malik, Stephan Sprengel, et al.

Ruijun Wang, Muhammad Muneeb, Anton Vasiliev, Aditya Malik, Stephan Sprengel, Gerhard Boehm, Ieva Simonyte, Augustinas Vizbaras, Kristijonas Vizbaras, Roel Baets, Markus-Christian Amann, Gunther Roelkens, "III-V/silicon photonic integrated circuits for spectroscopic sensing in the 2 $\mu$ m wavelength range," Proc. SPIE 10536, Smart Photonic and Optoelectronic Integrated Circuits XX, 1053603 (22 February 2018); doi: 10.1117/12.2287380

**SPIE.**

Event: SPIE OPTO, 2018, San Francisco, California, United States

## III-V/silicon photonic integrated circuits for spectroscopic sensing in the 2 $\mu\text{m}$ wavelength range

Ruijun Wang<sup>a,b,\*</sup>, Muhammad Muneeb<sup>a,b</sup>, Anton Vasiliev<sup>a,b</sup>, Aditya Malik<sup>a,b</sup>, Stephan Sprengel<sup>c</sup>, Gerhard Boehm<sup>c</sup>, Ieva Šimonytė<sup>d</sup>, Augustinas Vizbaras<sup>d</sup>, Kristijonas Vizbaras<sup>d</sup>, Roel Baets<sup>a,b</sup>, Markus-Christian Amann<sup>c</sup>, Gunther Roelkens<sup>a,b</sup>

<sup>a</sup>Photonics Research Group, Ghent University-imec, Technologiepark-Zwijnaarde 15, 9052 Ghent, Belgium;

<sup>b</sup>Center for Nano- and Biophotonics (NB-Photonics), Ghent University, Ghent, Belgium;

<sup>c</sup>Walter Schottky Institut, Technische Universität München, Am Coulombwall 4, 85748 Garching, Germany;

<sup>d</sup>Brolis Semiconductors UAB, Moletu pl. 73, LT-14259, Vilnius, Lithuania

### ABSTRACT

III-V/silicon photonic integrated circuits (ICs) promise to enable low cost and miniature optical sensors for trace-gas detection, bio-sensing and environmental monitoring. A lot of these applications can benefit from the availability of photonic ICs beyond the telecommunication wavelength range. The 2  $\mu\text{m}$  wavelength range is of interest for spectroscopic detection of many important gases and blood constituents. In this contribution we will present 2  $\mu\text{m}$ -wavelength-range III-V/silicon photonic ICs consisting of tunable laser sources, photodetectors and silicon waveguide circuits. Silicon waveguides with a loss of  $\sim 0.5$  dB/cm are obtained in a well-established silicon photonics platform. Based on the waveguides, low insertion loss (2-3 dB) and low crosstalk (25-30 dB) arrayed waveguide gratings (AWGs) are realized for the 2.3  $\mu\text{m}$  wavelength range. Active opto-electronic components are integrated on the photonic IC by the heterogeneous integration of an InP-based type-II epitaxial layer stack on silicon. III-V-on-silicon 2.3  $\mu\text{m}$  range distributed feedback (DFB) lasers can operate up to 25  $^{\circ}\text{C}$  in continuous-wave regime and shows an output power of 3 mW. By varying the silicon grating pitch, a DFB laser array with broad wavelength coverage from 2.28  $\mu\text{m}$  to 2.43  $\mu\text{m}$  is achieved. III-V-on-silicon photodetectors with the same epitaxial layer stack exhibit a responsivity of 1.6 A/W near 2.35  $\mu\text{m}$ . In addition, we also report a 2  $\mu\text{m}$  range GaSb/silicon hybrid external cavity laser using a silicon photonic IC for wavelength selective feedback. A wavelength tuning over 58 nm and side mode suppression ratio better than 60 dB is demonstrated.

**Keywords:** Silicon Photonics, Mid-Infrared, photodetector, arrayed waveguide grating, spectroscopic sensing

### 1. INTRODUCTION

Silicon photonics has received great interest as a promising integrated-optics platform for various applications in the telecommunication wavelength range, such as optical interconnects [1,2]. This platform can take advantage of the silicon electronics processes to fabricate photonic devices in high yield and high volume. In addition, the high refractive index contrast of silicon-on-insulator (SOI) waveguides enables a tight bending radius, and consequently ultra-compact photonic devices and systems. With these advantages, in recent years the potential applications of silicon photonic integrated circuits (ICs) are extended to spectroscopic sensing [3-5]. However, the silicon photonic devices used at telecommunication wavelengths are typically retained for most of these new applications due to the lack of components at other wavelengths [6-8], which limits the performance of these silicon photonics sensing systems.

The 2  $\mu\text{m}$  wavelength range is of interest for security, environmental and process control applications since many important gases have strong absorption lines in this wavelength range [9]. The availability of silicon photonic ICs in the 2  $\mu\text{m}$  wavelength range enables miniature optical sensors for trace gas sensing. Besides, it is also valuable for bio-sensing applications, such as blood glucose measurements [10]. In these applications, the silicon photonic spectroscopic sensor should have a light source, a probe component and a spectrometer or single pixel detector. Silicon is an indirect bandgap semiconductor with extremely low light emission efficiency, transparent beyond 1.1  $\mu\text{m}$  wavelength. In order to

realize fully integrated silicon photonic systems for the 2  $\mu\text{m}$  wavelength range, a lot of effort has been devoted to integrate 2  $\mu\text{m}$ -wavelength-range active photonic devices on silicon [11-20]. In this contribution, we present the development of fully integrated III-V-on-silicon photonic circuits for spectroscopic sensing applications in the 2  $\mu\text{m}$  wavelength range.

## 2. III-V-ON-SILICON PLATFORM FOR THE 2 $\mu\text{m}$ WAVELENGTH RANGE

In most applications, a spectroscopic sensing system should have a light source, a probe component and a spectrometer or single pixel detector. Figure 1 shows two typical configurations for fully integrated silicon photonics on-chip spectroscopic sensors [5]. In both configurations, light is coupled from the integrated light source to the waveguide and then split to two arms. The probe component in one arm interacts with environment while the other one provides the reference information. In the case of liquid sensing, a low-cost broadband light source such as a light emitting diode (LED) can be used since liquid samples typically have broad absorption features. In this configuration, a spectrometer with integrated photodetectors should be implemented to analyze the absorption spectra. For gas sensing, typically a tunable single mode laser is required to probe the absorption lines of gases, as used in the popular tunable diode laser absorption spectroscopy (TDLAS) technique. Integrating a widely tunable laser or a broadband wavelength coverage laser array on the waveguide circuit enables to simultaneously detect several gases or even broad absorption features of liquids using the configuration shown in Fig. 1(b).

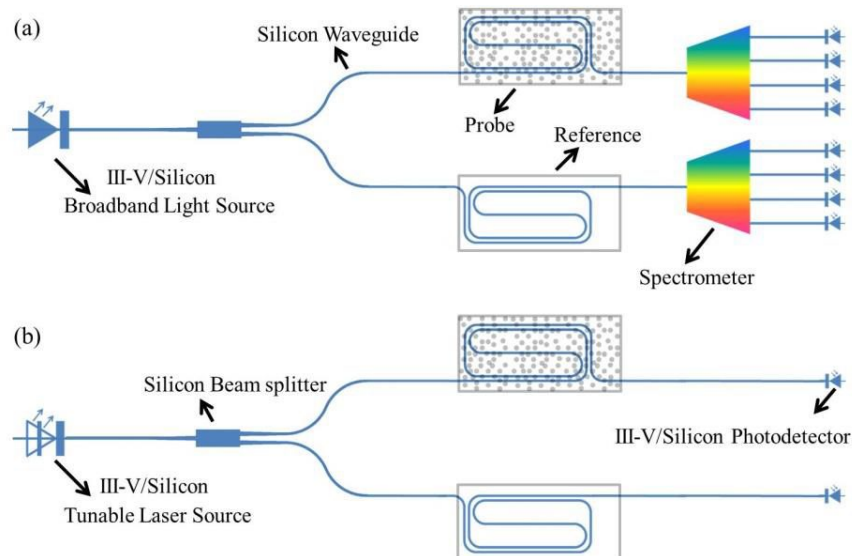


Figure 1. Schematic of two silicon photonic configurations to realize an integrated on-chip absorption spectroscopy sensor. (a) Broadband source and spectrometer, best suited for liquid and solid analytes; (b) tunable single mode laser source for trace gas detection.

We realized heterogeneously integrated III-V-on-silicon lasers and photodetectors by adhesively bonding an InP-based type-II epitaxial layer stack on silicon. Figure 2(a) shows the schematic cross-section of the heterogeneous InP-based type-II device on a SOI waveguide. The III-V epitaxial layer stack is adhesively bonded to a SOI waveguide using an ultra-thin divinylsiloxane-benzocyclobutene (DVS-BCB) layer of a few tens of nanometers. After bonding, the InP-substrate is removed by HCl wet etching. Then the lasers and photodetectors are co-processed on the III-V membrane. First, an anisotropic HCl wet etch of the *p*-InP cladding layer is employed to create a “V”-shaped mesa. Then the active region is etched by using a 1:1:20:70  $\text{H}_3\text{PO}_4:\text{H}_2\text{O}_2:\text{citric acid}:\text{H}_2\text{O}$  solution. Subsequently, the devices are isolated by wet etching of the *n*-InP layer using HCl. A combination of  $\text{SiN}_x$  and DVS-BCB is used to passivate the device mesa. A scanning electron microscopy (SEM) image of the cross-section of the fabricated III-V-on-silicon devices is shown in Fig. 2(b).

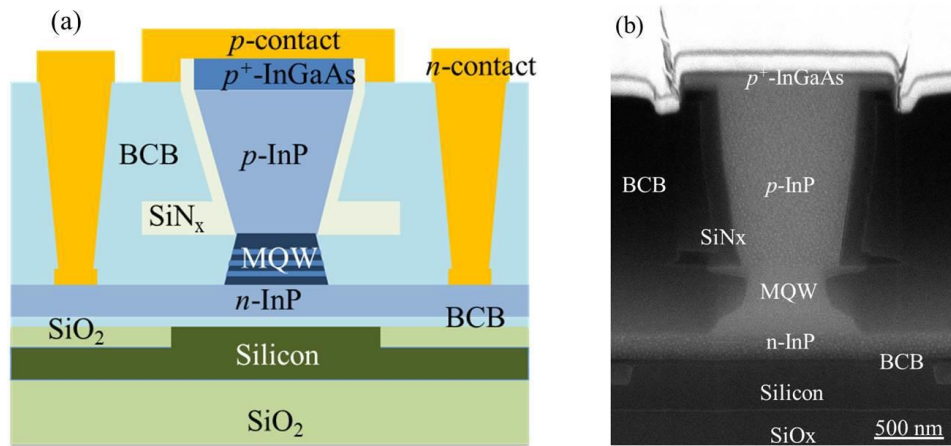


Figure 2. (a) Schematic drawing and (b) SEM image of the cross section of a heterogeneously integrated III-V-on-silicon type-II active device.

### 3. III-V-ON-SILICON PHOTODETECTORS AND SPECTROMETERS

For a waveguide-based optical sensor, photodetectors should be integrated with the waveguide circuits to convert the optical signals to an electrical response. We study III-V-on-silicon photodetectors based on two different coupling methods between the III-V active region and the silicon waveguide: adiabatically-coupled and grating-assisted photodetectors [12,13]. In the first structure, light is efficiently coupled from the silicon waveguide into the III-V waveguide by a narrow taper tip, and subsequently absorbed by the active region, as schematically shown in Fig. 3(a). Figure 3(b) shows the I-V curve of the adiabatically-coupled photodetector under different waveguide-referred input power levels at 2.35  $\mu\text{m}$  wavelength. A responsivity of 1.6 A/W at 2.35  $\mu\text{m}$  wavelength and dark current of 10 nA at  $-0.5$  V can be extracted from the curve. In the grating-assisted photodetector, light in the silicon waveguide is diffracted to the III-V active region by using a silicon grating. This type of photodetector shows a responsivity of 0.1 A/W and dark current of 5 nA at  $-0.5$  V.

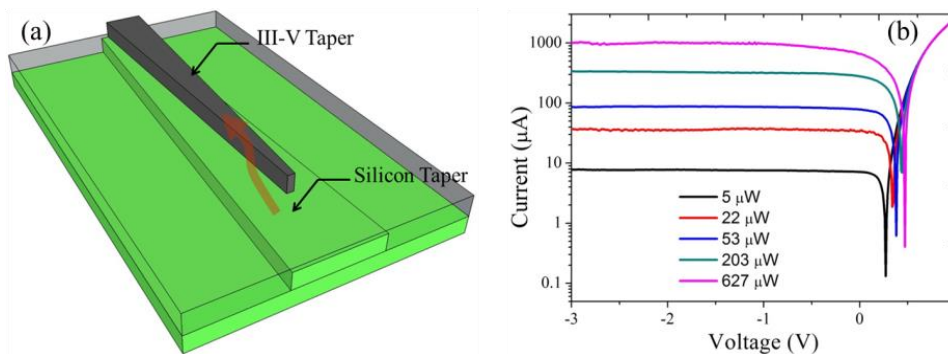


Figure 3. (a) Schematic of an adiabatically-coupled photodetector integrated on a silicon waveguide; (b) I-V curve of the photodetector under different waveguide-coupled input powers at a wavelength of 2.35  $\mu\text{m}$ .

Arrayed waveguide gratings (AWGs) are widely used as (de)multiplexers in wavelength division multiplexing systems and can also be used as spectrometers in spectroscopic sensors [13]. Figure 4(a) displays a microscope image of a 2.3  $\mu\text{m}$  AWG spectrometer integrated with an adiabatically-coupled InP-based type-II quantum well photodetector array. Before heterogeneous integration with III-V photodetectors, the passive AWG spectrometer has an insertion loss of 2.5 dB and a crosstalk level of  $-30$  dB. Figure 4(b) shows the photo-response of the 2.3  $\mu\text{m}$  III-V-on-silicon spectrometer. An insertion loss of 3 dB and crosstalk level of  $-27$  dB is obtained by normalizing the responsivity to the reference

photodetector. This result indicates that the bonding of III-V material on silicon and related post-processes do not degrade the performance of the AWG spectrometer.

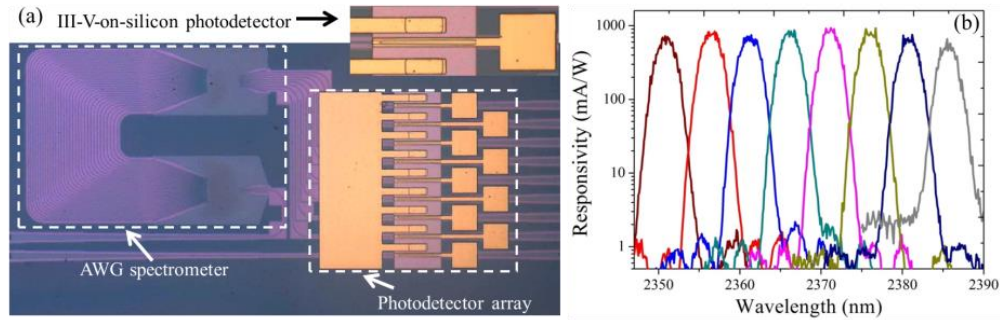


Figure 4. (a) Microscope image of a 2.3  $\mu\text{m}$  AWG spectrometer integrated with a InP-based type-II quantum well photodetector array; (b) photo-response of the 2.3  $\mu\text{m}$  III-V-on-silicon AWG spectrometer.

#### 4. III-V-ON-SILICON 2.3 $\mu\text{m}$ -WAVELENGTH-RANGE LASERS

Using the same epitaxial layer stack as for the heterogeneously integrated InP-based type-II photodetectors, 2  $\mu\text{m}$  wavelength range III-V-on-silicon Fabry-Perot lasers and distributed feedback (DFB) lasers are realized. Figure 5(a) shows the schematic of a III-V-on-silicon Fabry-Perot laser [15]. The device consists of a gain section, a III-V/silicon spot size converter (SSC) on both sides and two silicon Bragg grating reflectors (DBRs) to form the laser cavity. An efficient light coupling from the III-V waveguide to the silicon waveguide is realized using the III-V/silicon SSCs. In continuous-wave (CW) operation, a threshold current density of 2.7  $\text{kA}/\text{cm}^2$  and output power of 1.3 mW at 5  $^\circ\text{C}$  is achieved for the Fabry-Perot laser. The laser emits over 3.7 mW of peak power with a threshold current density of 1.6  $\text{kA}/\text{cm}^2$  in pulsed regime at room temperature. A high-resolution emission spectrum of the Fabry-Perot laser is shown in Fig. 5(b).

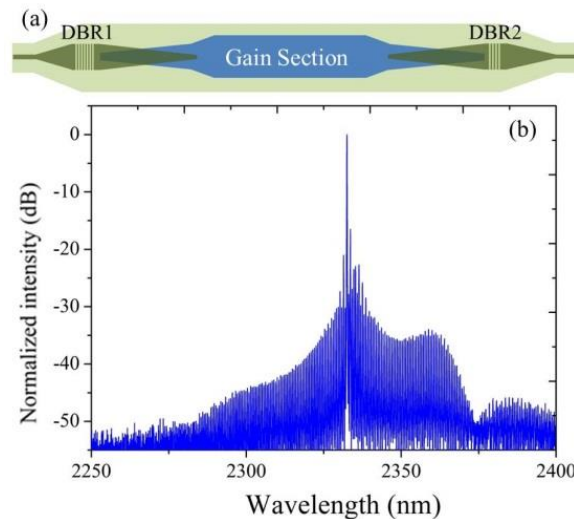


Figure 5. (a) Schematic of a III-V-on-silicon Fabry-Perot laser; (b) fiber-coupled emission spectrum of a heterogeneously integrated InP-based type-II Fabry-Perot laser.

DFB lasers are well-suited light sources for the TDLAS measurement of gases. Figure 6(a) shows the schematic of an InP-based type-II DFB laser heterogeneously integrated on a silicon waveguide [16]. A quarter-wave shifted first-order

DFB grating with an etch depth of 180 nm in a 400 nm silicon device layer are implemented beneath the gain section. The evanescent tail of the optical mode interacts with this grating, which selects the lasing wavelength of the DFB laser. In CW regime, the heterogeneously integrated InP-based type-II DFB laser can operate up to 25 °C and emits more than 3 mW output power in a single mode with a threshold current density of 1.8 kA/cm<sup>2</sup> at 5 °C. The lasing wavelength of the III-V-on-silicon DFB lasers is determined by the silicon grating pitch. Figure 6(b) shows the emission spectra of six 1000 μm-long heterogeneously integrated DFB lasers in an array [18]. As the silicon grating pitch increases from 343 nm to 368 nm, the lasing wavelength shifts from 2280 nm to 2430 nm. This broad wavelength span overlaps with absorption features of several important gases, such as NH<sub>3</sub>, CO, CH<sub>4</sub>, C<sub>2</sub>H<sub>2</sub> and HF. Besides adjusting the grating pitch, another method to control the lasing wavelength is to adjust the gain section width of the DFB lasers. Figure 6(c) shows the CW lasing spectra of four 700 μm-long DFB lasers with different III-V waveguide widths as a function of bias current. More than 10 nm continuous current-tuning range is achieved this way. We carried out a CO gas sensing measurement using a III-V-on-silicon DFB laser source. It can be seen from Fig. 6(d) that the measurement result fits very well to data from the HITRAN database.

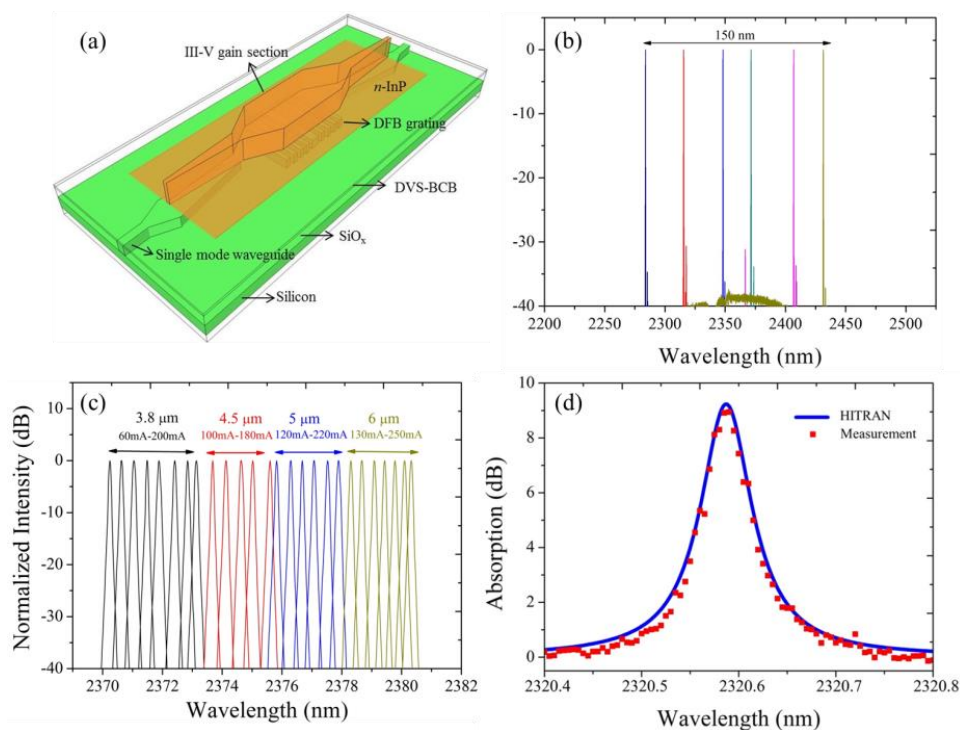


Figure 6. (a) Schematic of a heterogeneously integrated InP-based type-II DFB laser on silicon; emission spectrum of a DFB laser array with varied silicon grating period (b) and varied III-V waveguide width (c); (d) direct TDLAS measurement of CO using a III-V-on-silicon DFB laser source and the corresponding HITRAN spectrum.

## 5. GASB/SILICON HYBRID EXTERNAL CAVITY LASER

We also realized a GaSb/silicon hybrid external cavity laser by butt coupling a GaSb-based gain chip and a silicon photonic IC [17]. The silicon photonic IC contains a Vernier filter consisting of two thermally tuned micro-ring resonators (MRRs), a phase section to allow for quasi-continuous wavelength tuning and a DBR as shown in Fig. 7(a). Fig. 7(b) shows the superimposed lasing spectra of the GaSb/silicon hybrid laser by tuning one MRR. A tuning range of 58 nm is achieved with a SMSR better than 52 dB over the full tuning range and more than 60 dB at the optimal wavelength. When only one MRR is tuned, the tuning resolution is determined by the FSR of the other MRR. Fine

quasi-continuous wavelength tuning can be achieved by simultaneously tuning both MRRs. Fig. 7(c) shows the superimposed spectra with 0.7 nm resolution tuning over 25 nm range realized in this way. But even when tuning both MRRs, the tuning resolution is still limited by the FSR of the longitudinal modes of the Fabry-Perot cavity. Continuous tuning can be achieved by thermally tuning the phase section as shown in Fig. 7 (d). As the coupling gap of the MRRs increases from 200 nm to 500 nm, the maximum output power of the GaSb/silicon hybrid laser reduces from 7.5 mW to 3.8 mW. But the SMSR and tuning smoothness are lowered as the coupling gap is reduced.

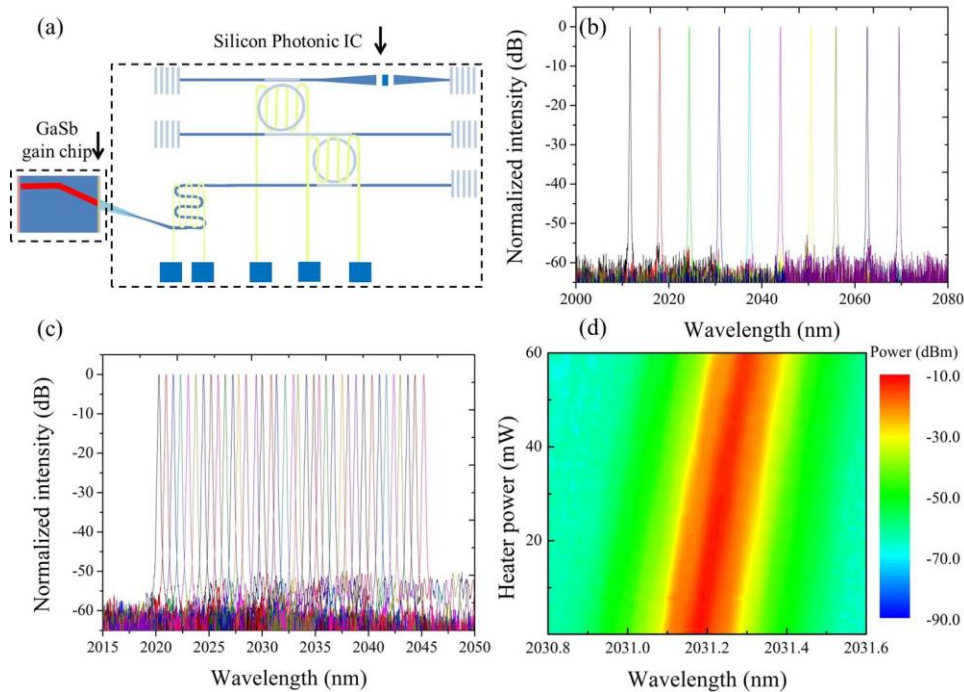


Figure 7. (a) Schematic of a GaSb/silicon hybrid external cavity laser; superimposed spectra of the laser by thermally tuning one MRR (b), two MRRs (c) and phase shifter (d) when the coupling gap of MRRs is 500 nm.

## 6. CONCLUSION

In this paper, we report fully integrated 2  $\mu\text{m}$ -wavelength-range III-V-on-silicon photonic circuits consisting of silicon waveguides, laser sources, photodetectors and AWG spectrometers. The active opto-electronic photonic devices are realized by heterogeneously integrating a InP-based type-II epitaxial layer stack on silicon waveguides. In addition, a widely tunable GaSb/silicon hybrid external cavity laser by combing a GaSb-based gain chip and a silicon photonics IC is reported.

## REFERENCES

- [1] Vivien, L. and Pavesi, L., "Handbook of Silicon Photonics," Taylor & Francis, 2013.
- [2] Miller, D.A.B., "Device requirements for optical interconnects to silicon chips," IEEE Proc. 97, 1166–1185 (2009).
- [3] Subramanian, A., Ryckeboer, E. M. P., Dhakal, A., Peyskens, F., Malik, A., Kuyken, B., Zhao, H., Pathak, S., Ruocco, A., De Groote, A., Wuytens, P. C., Martens, D., Leo, F., Xie, W., Dave, U. D., Muneeb, M., Dorpe, P. V., Campenhout, J. V., Bogaerts, W., Bienstman, P., Thomas, N. L., Thourhout, D. V., Hens, Z., Roelkens, G. and Baets, R., "Silicon and silicon nitride photonic circuits for spectroscopic sensing on-a-chip," Photonics Research 5(3), 47–59 (2015).

- [4] Tombez, L., Zhang, E. J., Orcutt, J. S., Kamlapurkar, S. and Green, W. M. J., "Methane absorption spectroscopy on a silicon photonic chip," *Optica* 4(11), 1322-1325 (2017).
- [5] Wang, R., Vasiliev, A., Muneeb, M., Malik, A., Sprengel, S., Boehm, G., Amann, M.-C., Šimonytė, I., Vizbaras, A., Vizbaras, K., Baets, R. and Roelkens, G., "III-V-on-Silicon Photonic Integrated Circuits for Spectroscopic Sensing in the 2–4  $\mu\text{m}$  Wavelength Range," *Sensors* 17, 1788- (2017).
- [6] Spott, A., Stanton, E.J., Volet, N., Peters, J.D., Meyer, J.R. and Bowers, J.E., "Heterogeneous Integration for Mid-Infrared Silicon Photonics," *IEEE J. Sel. Top. Quantum Electron.* 23, 8200810(2017).
- [7] Lin, H., Luo, Z., Gu, T., Kimerling, L.C., Wada, K., Agarwal, A. and Hu, J., "Mid-infrared integrated photonics on silicon: a perspective," *Nanophotonics*, 7(2), 393-420 (2017).
- [8] Hu, T., Dong, B., Luo, X., Liow, T.Y., Song, J., Lee, C. and Lo, G.Q., "Silicon photonic platforms for mid-infrared applications," *Photonics Research*, 5(5), 417-430 (2017).
- [9] Rothman, L., Gordon, I., Babikov, Y., Barbe, A., Benner, D.C., Bernath, P., Birk, M., Bizzocchi, L., Boudon, V., Brown, L., et al., "The HITRAN 2012 molecular spectroscopic database," *J. Quant. Spectrosc. Radiat. Transf.* 130, 4–50 (2013).
- [10] Alexeeva, N.V. and Arnold, M.A., "Near-infrared microspectroscopic analysis of rat skin tissue heterogeneity in relation to noninvasive glucose sensing," *J. Diabetes Sci. Technol.* 3, 219 (2009).
- [11] Ackert, J.J., Thomson, D.J., Shen, L., Peacock, A.C., Jessop, P.E., Reed, G.T., Mashanovich, G.Z. and Knights, A.P., "High-speed detection at two micrometres with monolithic silicon photodiodes," *Nature Photonics*, 9(6), 393-396 (2015).
- [12] Wang, R., Muneeb, M., Sprengel, S., Boehm, G., Malik, A., Baets, R., Amann, M.C. and Roelkens, G., "III-V-on-silicon 2- $\mu\text{m}$ -wavelength-range wavelength demultiplexers with heterogeneously integrated InP-based type-II photodetectors," *Optics express*, 24(8), 8480-8490 (2016).
- [13] Wang, R., Sprengel, S., Muneeb, M., Boehm, G., Baets, R., Amann, M.C. and Roelkens, G., "2  $\mu\text{m}$  wavelength range InP-based type-II quantum well photodiodes heterogeneously integrated on silicon photonic integrated circuits," *Optics express*, 23(20), 26834-26841(2015).
- [14] Spott, A., Davenport, M., Peters, J., Bovington, J., Heck, M.J., Stanton, E.J., Vurgaftman, I., Meyer, J. and Bowers, J., "Heterogeneously integrated 2.0  $\mu\text{m}$  CW hybrid silicon lasers at room temperature," *Optics letters*, 40(7), 1480-1483 (2105).
- [15] Wang, R., Sprengel, S., Boehm, G., Muneeb, M., Baets, R., Amann, M.C. and Roelkens, G., "2.3  $\mu\text{m}$  range InP-based type-II quantum well Fabry-Perot lasers heterogeneously integrated on a silicon photonic integrated circuit," *Optics express*, 24(18), 21081-21089 (2016).
- [16] Wang, R., Sprengel, S., Malik, A., Vasiliev, A., Boehm, G., Baets, R., Amann, M.C. and Roelkens, G., "Heterogeneously integrated III-V-on-silicon 2.3x  $\mu\text{m}$  distributed feedback lasers based on a type-II active region," *Applied Physics Letters*, 109(22), 221111 (2016).
- [17] Wang, R., Malik, A., Šimonytė, I., Vizbaras, A., Vizbaras, K. and Roelkens, G., "Compact GaSb/silicon-on-insulator 2.0 x  $\mu\text{m}$  widely tunable external cavity lasers," *Optics express*, 24(25), 28977-28986 (2016).
- [18] Wang, R., Sprengel, S., Boehm, G., Baets, R., Amann, M.C. and Roelkens, G., "Broad wavelength coverage 2.3  $\mu\text{m}$  III-V-on-silicon DFB laser array," *Optica*, 4(8), 972-975 (2017).
- [19] Wirths, S., Geiger, R., Von Den Driesch, N., Mussler, G., Stoica, T., Mantl, S., Ikonik, Z., Luysberg, M., Chiussi, S., Hartmann, J.M. and Sigg, H., "Lasing in direct-bandgap GeSn alloy grown on Si," *Nature photonics*, 9(2), 88 (2015).
- [20] Volet, N., Spott, A., Stanton, E.J., Davenport, M.L., Chang, L., Peters, J.D., Briles, T.C., Vurgaftman, I., Meyer, J.R. and Bowers, J.E., "Semiconductor optical amplifiers at 2.0- $\mu\text{m}$  wavelength on silicon," *Laser & Photonics Reviews*, 11(2), 1600165 (2107).